Supporting information

Photoluminiscent 1-2 nm size silicon nanoparticles: A surface-dependent system.

Juan J. Romero[a], Manuel J. Llansola-Portolés[a†], María Laura Dell´Arciprete[a], Hernán B. Rodríguez[a], Ana L. Moore[b], Mónica C. Gonzalez.[a*]

[a] *Instituto de Investigaciones Fisicoquímicas Teóricas y Aplicadas (INIFTA), Facultad de Ciencias Exactas, Universidad Nacional de La Plata, Casilla de Correo 16, Sucursal 4, (1900) La Plata, Argentina. E-mail: gonzalez@inifta.unlp.edu.ar.*

[b] *Department of Chemistry and Biochemistry, Center for Bioenergy and Photosynthesis, Arizona State University, Tempe, Arizona 85287-1604, USA.*

** E-mail: gonzalez@inifta.unlp.edu.ar*

† Present address: Department of Chemistry and Biochemistry, Center for Bioenergy and Photosynthesis, Arizona State University, Tempe, Arizona 85287-1604, USA.

S.I. Characterization

TDSiNPs:

TEM micrographs of small particle agglomerates showing the lattice fringes.

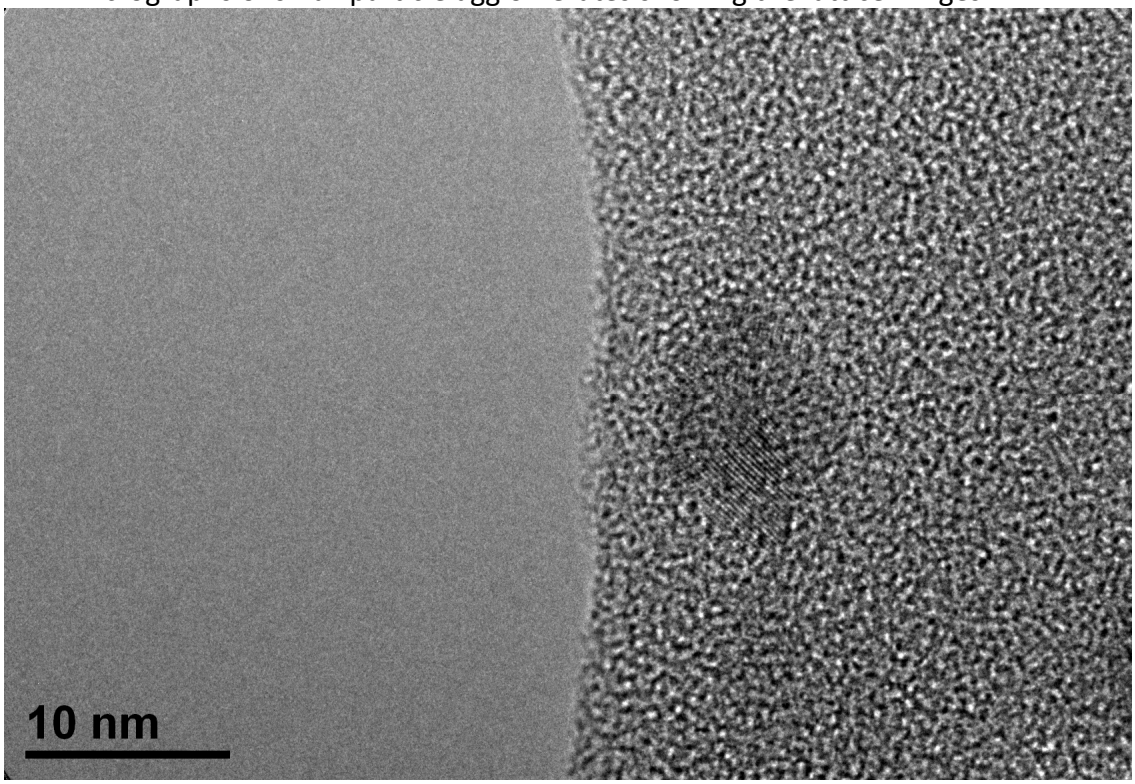

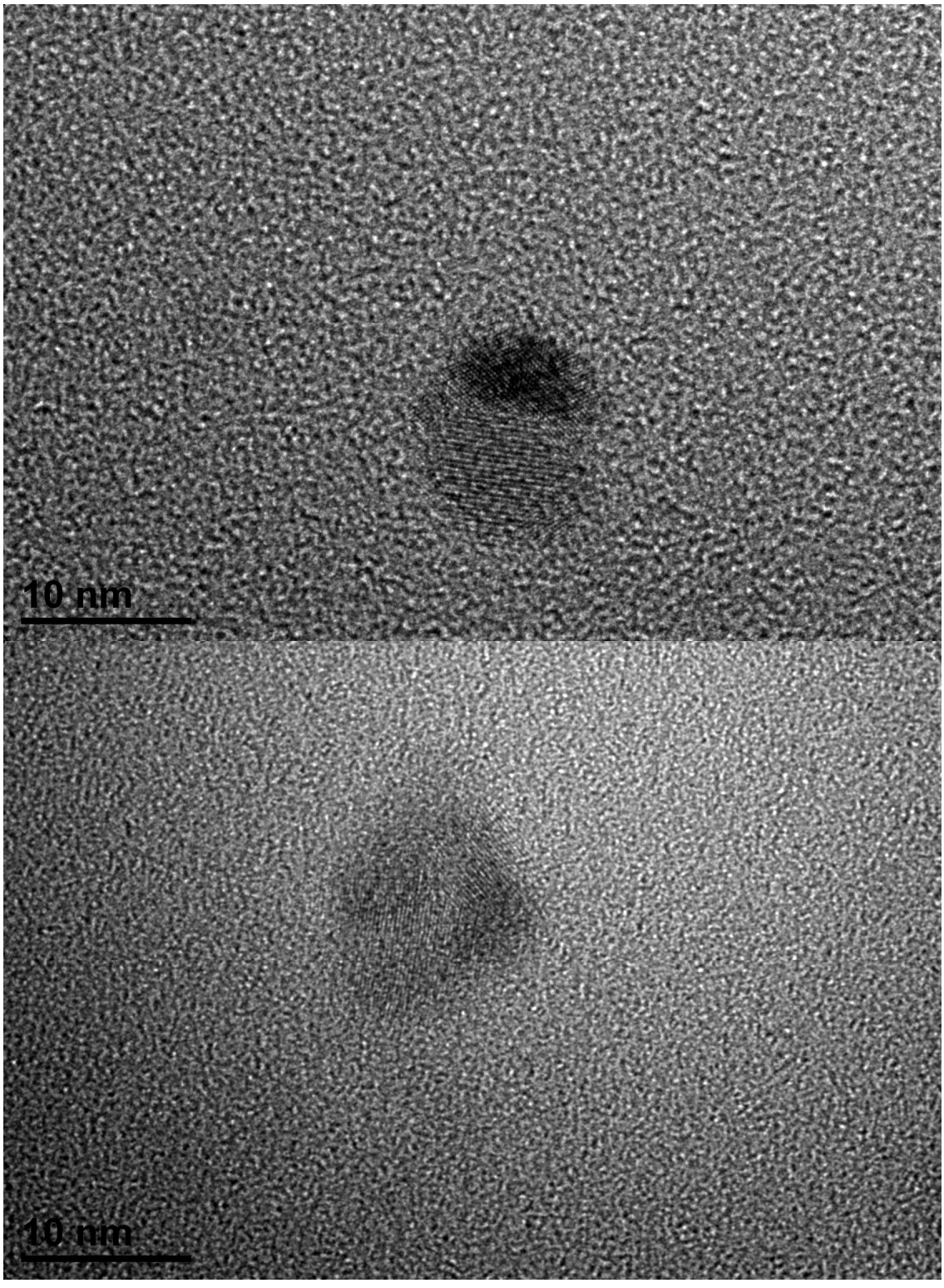
10 nm
10 nm

BUSiNPs:

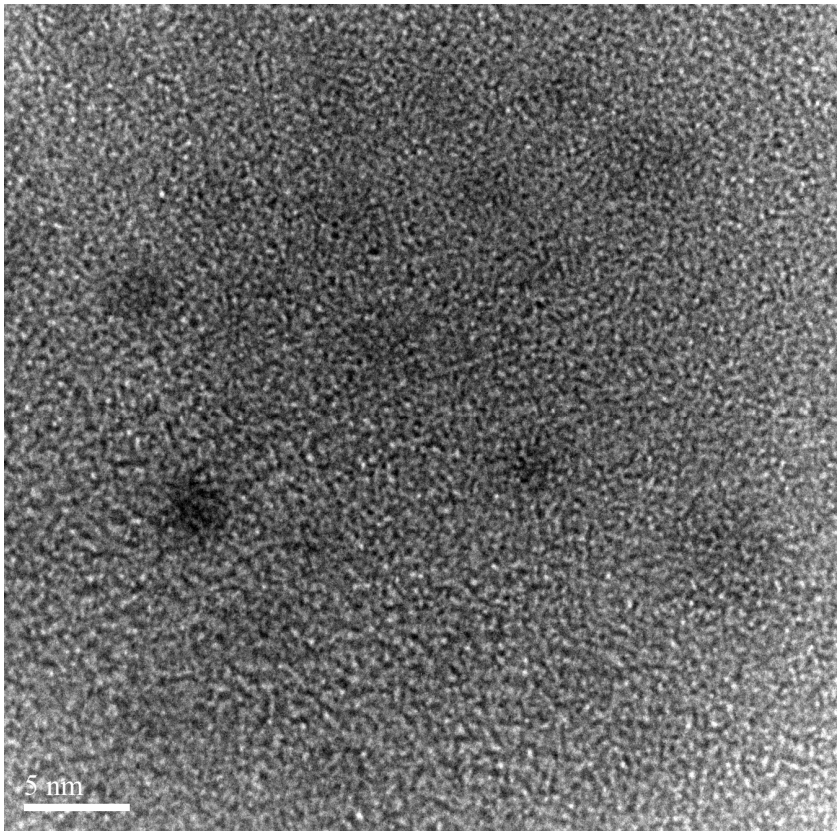

PASiO$_x$-TDSiNPs:

Using the survey spectra, and taking into account a correction for adventitious carbon[1], the global composition obtained through XPS was **$Si_{12}C_{3.5}H_yN_1O_x$**.

Results from the high resolution XPS are shown in the next table.

Peak	RSF	B.E. (eV)	FWHM (eV)	Area (%)
C 1s	1	284.60	1.14	3723.59 (100)
Si 2p	0.865	101.7	0.99	259.15 (39.3)
		102.6	1.29	399.78 (60.7)
O 1s	2.85	531.9	1.78	3242.52 (100)
N 1s	1.77	399.4	2.02	3445.76 (100)

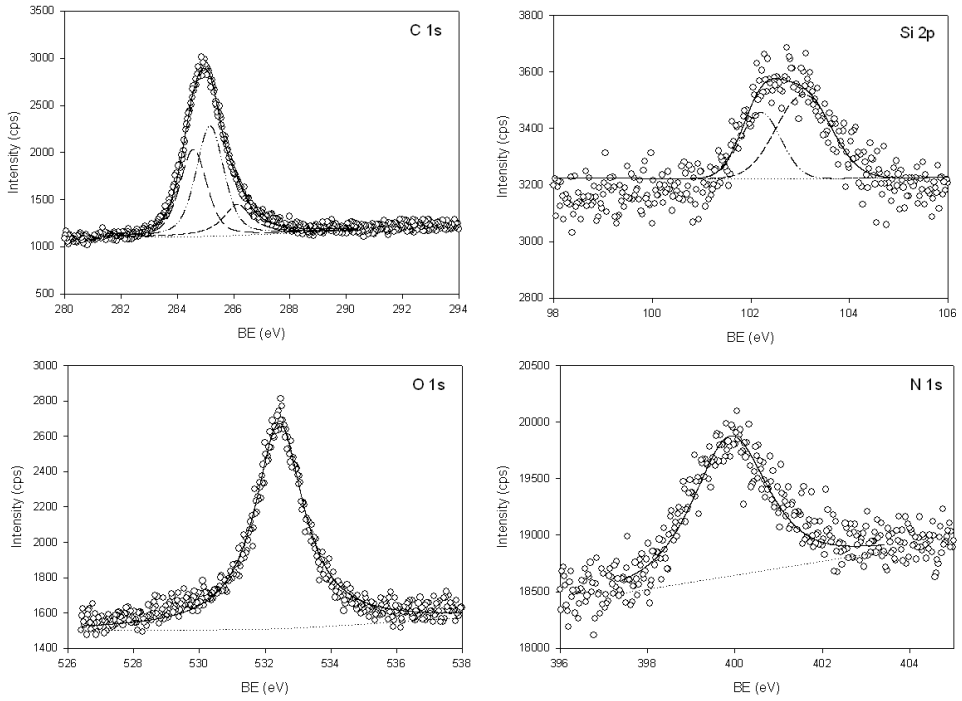

PA-TDSiNPs:

Using the survey spectra, and taking into account a correction for adventitious carbon,[1] the global composition obtained through XPS was $\mathbf{Si_2C_5N_{4.4}H_y}$.

Results from the high resolution XPS are shown in the next table.

Peak	RSF	B.E. (eV)	FWHM (eV)	Area (%)
C 1s	1	284.6	1.78	3419.88 (100)
Si 2p	0.865	99.70	1.28	179.64 (9.5)
		100.70	148	1082.84 (56.7)
		101.8	1.96	646.17 (33.8)
O 1s	2.85	531.35	1.55	1574.31 (54.4)
		532.00	1.40	1317.68 (45.6)
N 1s	1.77	399.40	2.28	4079.77 (100)

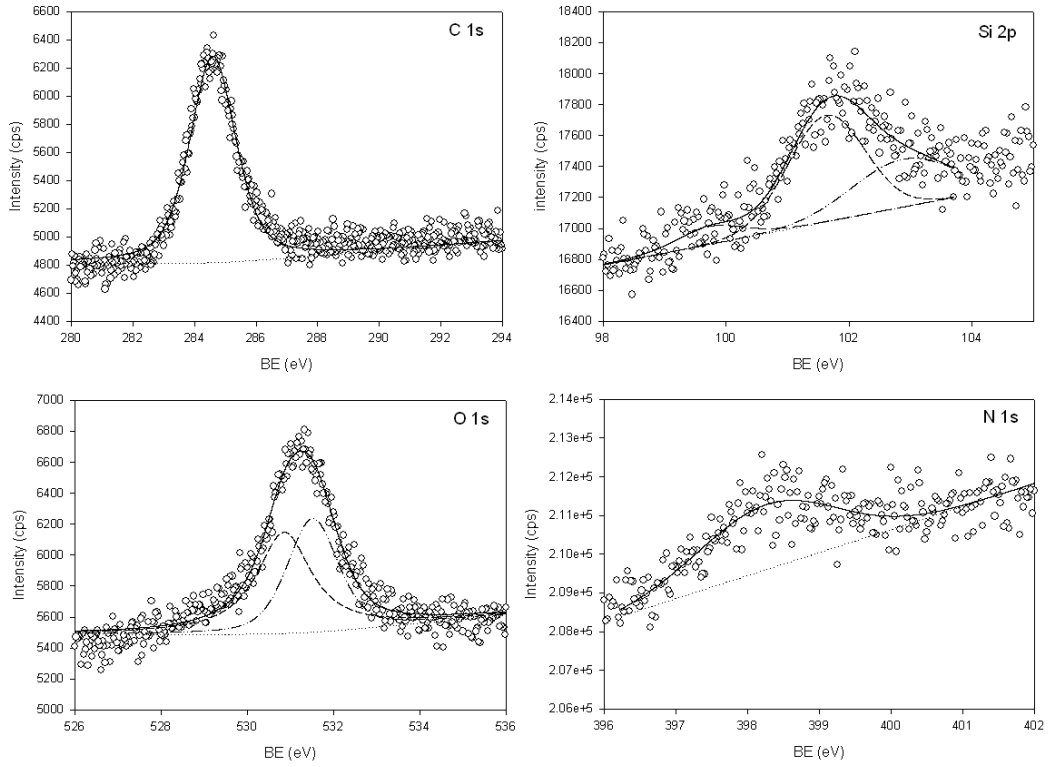

PA-BUSiNPs

The FTIR spectra of PA-TDSiNPs (blue traces) and PA-BUSiNPs (red traces), obtained in KBr pellets as support, are shown in the following figure. The vertical solid lines stand as guides to the eye for the peak positions. Both compounds show the presence of bands at 1460 and 733 cm^{-1} due to Si-C deformation and CH_2 rocking in Si-CH_2 respectively, as well as peaks in the 2970 – 2880 cm^{-1} region due to CH_2 stretching and bending, confirming PA bonding to SiNPs.[2,3] A small absorption at 850 cm^{-1} could be assigned to the presence of Si-N vibrations. [4]

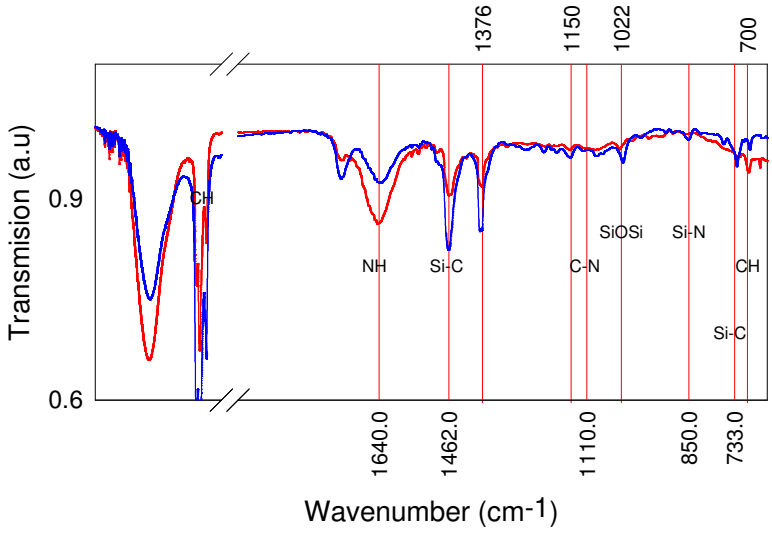

The corresponding XPS spectrum of PA-BUSiNPs shows Si 2p signals at 101.5 eV (45%) and 102.2 eV (55%) characteristic of Si(C_xN_y) environments.[5,6] The 398.5 eV N 1s signal characteristic of N-Si environments further supports the presence of Si-N bonds.[7] As already discussed, N-bonding to Si may be a secondary product of the radical mechanism involved in the synthesis reaction, as described in S.I. Scheme 1.

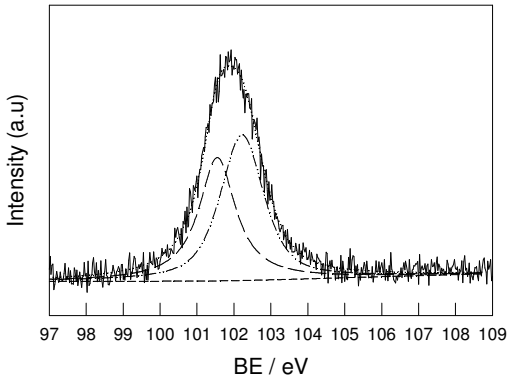

SiO_x-BUSiNPs and $PASiO_x$-BUSiNPs

The FTIR spectra of SiO_x-SiNPs and $PASiO_x$-SiNPs are shown in S.I. Fig. 1A. SiO_x-SiNPs spectrum shows a weak broad absorption band around 3400 cm^{-1} which could be attributed to H-bonded Si-OH groups, a more intense broad band at 1068 cm^{-1} and a peak at 968 cm^{-1}, both characteristic of Si-O-Si stretching. [8] Other observed peaks are due to remnant amounts of surface adsorbed TOAB used as a surfactant during the synthesis procedure. On the other hand, the FTIR spectrum of $PASiO_x$-SiNPs show a weak broad absorption band around 3280 cm^{-1}, in coincidence with that observed for (3- aminopropyl)triethoxysilane, which is therefore assigned to the $–NH_2$ group. The narrow but more intense bands at 1162, 1122, 1040, and 970 cm^{-1} observed after derivatization of SiNPs, may indicate different Si-O-Si environments.[2] In fact, NH_2-SiNPs synthesis involved the reaction of surface silanols with APTES leading to a SiO_x shell, as shown in Scheme 1. The absence of bands around 1160 cm^{-1} and 1250 cm^{-1} due to symmetric Si-O-Si in bulk SiO_2 and Si=O vibrations, respectively, supports a negligible formation of SiO_2 structures in both, derivatized and underivatized particles. In fact, APTES derivatization is supported by the absorption bands at 1405, 1270, 720 and 750 cm^{-1} due to Si-C symmetric and

asymmetric deformation, stretching, and CH_2 rocking in Si-CH_2 respectively. Peaks due to CH_2 stretching and bending vibrations in the 2970 – 2880 cm^{-1} and 1440 – 1465 cm^{-1} region due to the propyl chain are also observed. Moreover, the absence of important broad bands around 760 and 1100 cm^{-1} due to Si-O-C characteristic of (3- aminopropyl)triethoxysilane IR spectrum (not shown) further supports a complete surface derivatization.[8]

S.I. Figure 1B shows the XPS spectrum obtained for PASiO_x-SiNPs and SiO_x-SiNPs (*inset*). The Si 2p region of both particles displays the contribution of silicon environments with binding energies (BE) of 100.1, 101.0, and 102.3 eV which may be assigned to Si^+, Si^{2+}, and Si^{3+} oxidized silicon, respectively, in $Si(-O-)_x$ and $Si(-Cl)_x$ coordinated compounds. Ratios between Si, O, and Cl signals corrected for the instrument sensitivity yield an average $Si_{4.2}O_{3.8}Cl$ surface composition for SiO_x-SiNPs, thus suggesting particle oxidation due to aging, in line with previous reported results. Silicon environments in PASiO_x-SiNPs depict BE attributable to Si^o, Si^+, Si^{2+}, and Si^{3+} oxidized silicon with less contribution of the more oxidized environments. Such behavior is in line with the protection ability towards oxidation of surface functionalities. Interestingly, the absence of peaks around 104 eV strongly suggests that amorphous SiO_2 coordination does not conform the particle structure. Therefore, XPS and FTIR data support aminopropyl functionalization as shown in Scheme 1.

S.I. Figure 1: (A) IR of (from top down) SiO_x-SiNPs and PASiO_x-SiNPs. (B) Si 2p XPS peaks observed for PASiO_x-SiNPs and SiO_x-SiNPs (*inset*).

(A) (B)

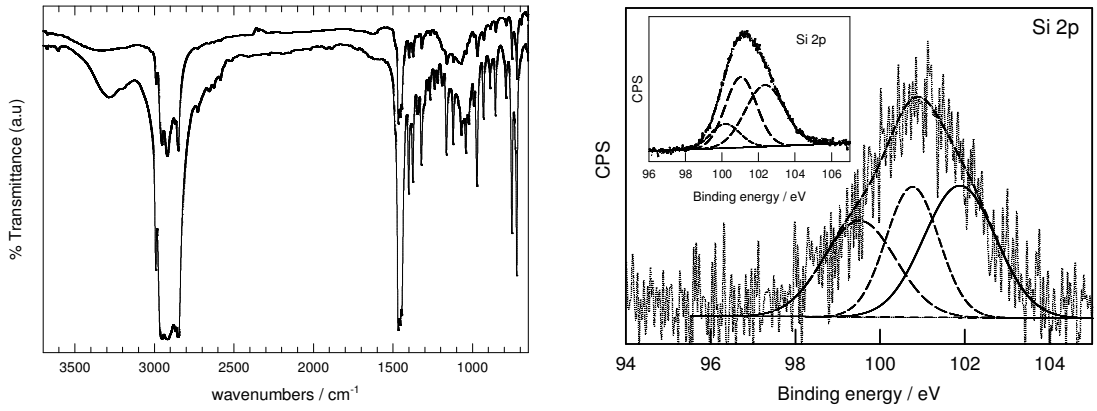

XPS Literature assignments:

Signal	Structure	B.E. (eV)	Reference
Si 2p	$Si(-O-)_4$	102.8 – 103.6	[9,10,11,12]
	$Si(-O-)_3$	102.0 – 102.8	
	$Si(-O-)_2$	101.4	
	$Si(-O-)_1$	100.6 – 100.0	
	Si-Si	99.2 – 99.0	[9,10,13]
	Si-H	99.6	[14,15]
	$Si(-H)_2$	100.8	[15]
	Si-C	100.4	
	$Si(C_xN_y)$	101.5 – 102.8	[5]
	Si-N	102.8	[7]
N 1s	$C-NH_2$	399.6 – 399.1	
O 1s	O-Si	535 [(a)]	[13]
	O-Si(H)	531.6[(a)]	

S.I. Scheme 1: Radical reaction mechanism taking place during the reaction of 2-propen 1-amine (AA) with Si-H surface groups to yield PA-TDSiNPs.

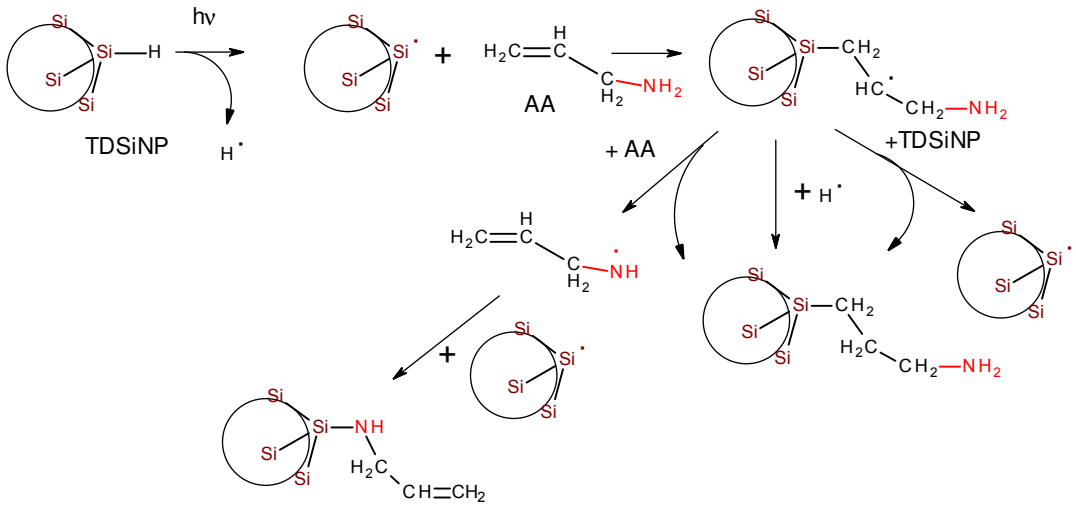

S.I. Table 1: Emission quantum efficiencies of argon-saturated $MASiO_x$-TD'SiNPs in toluene suspensions obtained at different temperatures. *n* and ε stand for the refractive index and relative permittivity of the solvent, respectively.

T (K)	ϕ	*n*	ε
273	0.90	1.537	2.438
283	0.83	1.531	2.41
293	0.76	1.524	2.40
303	0.69	1.519	2.37
313	0.62	1.512	2.34

The results show decreasing PL quantum yields with decreasing dielectric constant of toluene as a consequence of increased temperatures. Therefore, any contribution of the solvent to the thermal quenching is expected to be of little significance.

S.I. Surface Si atoms estimation

Geometry optimization was carried out using the density functional tight binding (DFTB) method with the aid of the DFTB+ program which allows SCC-DFTB calculations. Geometries are considered converged when the maximum element of the gradient vector of the energy with respect to nuclear coordinates is <0.01 au. The tolerance for charge self-consistency is fixed at 0.001 au. Nanoparticles containing between 17 and 240 silicon atoms in their core were modeled as spherical portions of crystalline bulk silicon, in which the Si−Si bond length is 2.36 Å. For mayor details, see publication by Llansola Portolés [16]. Because of the generation method, these particles resemble those obtained in a top-down procedure.

The figure in the right shows the optimized geometry, in vacuum at 0 K, for 1.3 nm size SiNPs with surface Si−H groups. Si groups not participating in Si-H bonds: yellow; Si groups participating in Si-H bonds: light brown; H, black. On the left is shown a vertical cut of the particle to show the inner silicon core.

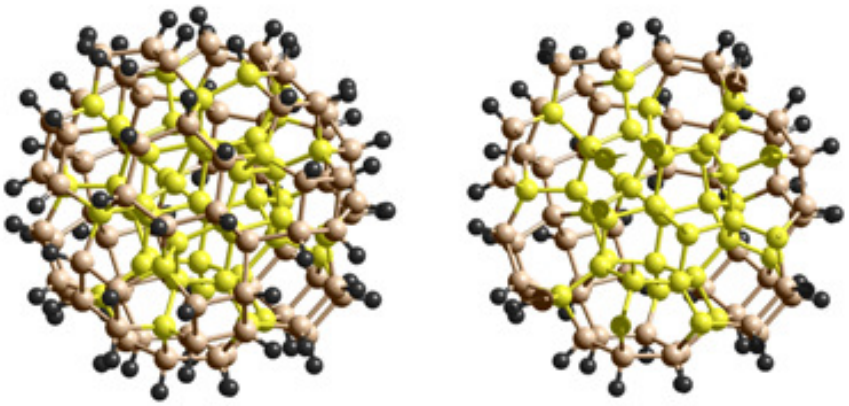

It is interesting to note, that 125 Si atoms conform the 1.3 nm size particle, from these, 74 atoms (59.2%) participate in Si-H bonds and another 15 Si atoms (12%) are exposed to the surface. Therefore, it may be consider that almost 71.2% of the Si atoms are in the surface.

Literature

(1) Payne, B. P.; Biesinger, M. C.; McIntyre, N. S. *J. Electron Spectrosc.* **2011**, *184*, 29.
(2) Launer, J. P. *MRS Bulletin* **1997**, *22*, 5.
(3) Wahab, M. A.; Kim, I.; Ha, C.-S. *J. Solid State Chem.* **2004**, *177*, 3439.
(4) Zhou, S.; Liu, W.; Cai, C.; Liu, H. Proc. SPIE 7995, Seventh International Conference on Thin Film Physics and Applications, **2011**, 79950T; doi: 10.1117/12.889047.
(5) Soto, G.; Samano, E. C.; Machorro, R.; Cota, L., *Vac. Sci. Technol.* **1998**, *16*, 1311-1315.
(6) *Silicon-Based Material and Devices*; Nalwa, H. S., Ed.; Academic Press: San Diego, 2001.
(7) Dasog, M.; Yang, Z.; Regli, S.; Atkins, T. M.; Faramus, A.; Singh, M. P.; Muthuswamy, E.; Kauzlarich, S. M.; Tilley, R. D.; Veinot, J. G. C. *ACS Nano* **2013**, *7*, 2676.
(8) Kluth, G. J.; Sung, M. M.; Maboudian, R. *Langmuir* **1997**, *13*, 3775.
(9) Wang, P. W.; Bater, S.; Zhang, L. P.; Ascherl, M.; Craig Jr, J. H. *Appl. Surf. Sci.* **1995**, *90*, 413.
(10) Ouyang, M.; Yuan, C.; Muisener, R. J.; Boulares, A.; Koberstein, J. T. *Chem. Mater.* **2000**, *12*, 1591.
(11) Zhu, Y.; Wang, H.; Ong, P. P. *Appl.Surf. Sci.* **2001**, *171*, 44.
(12) David Gara, P. M.; Garabano, N. I.; Llansola Portolés, M. J.; Moreno, S.; Dodat, D.; Casas, O. R.; Gonzalez, M. C.; Kotler, M. L. *J. Nanoparticles Res.* **2012**, *in press*.
(13) Yang, C. S.; Oh, K. S.; Ryu, J. Y.; Kim, D. C.; Shou-Yong, J.; Choi, C. K.; Lee, H. J.; Um, S. H.; Chang, H. Y. *Thin Solid Films* **2001**, *390*, 113.
(14) Hayashi, T.; Miyazaki, S.; Hirose, M. *Jap. J. Appl. Phys.* **1988**, *Part 2*, L314
(15) Nemanick, E. J.; Hurley, P. T.; Webb, L. J.; Knapp, D. W.; Michalak, D. J.; Brunschwig, B. S.; Lewis, N. S. *J. Phys. Chem. B* **2006**, *110*, 14770.
(16) Llansola Portolés, M. J.; Pis Diez, R.; Dell'Arciprete, M. L.; Caregnato, P.; Romero, J. J.; Mártire, D. O.; Azzaroni, O.; Ceolín, M.; Gonzalez, M. C. *J. Phys. Chem. C* **2012**, *116*, 11315.